tors (Γ_{11}'s). Parameter z_1^D in eq 4 is determined from $z_1^D = z - z_1^\alpha - z_1^\beta$ where z is the coordination number, here set equal to 10.
(39) Gehrke, S. H. *Kinetics of Gel Volume Change and Its Interaction with Solutes*; Ph.D. Thesis, University of Minnesota, 1986.
(40) Baker, J. P. *Polyacrylamide Copolymer Gels: Synthesis, Swelling, Microstructure*; M.S. Thesis, University of California, Berkeley, CA, 1989.
(41) Subroutine LMDIF from the MINPACK software library (Argonne National Laboratory, 9700 South Cass Ave., Argonne, IL 60439) was used for parameter optimization.
(42) Ball, R. C.; Doi, M.; Edwards, S. F.; Warner, M. *Polymer* **1981**, *22*, 1010.
(43) Shy, L. Y.; Eichinger, B. E. *J. Chem. Phys.* **1989**, *90*, 5179.

Registry No. (AAm)(MAPTAC)(BIS) (copolymer), 98587-56-5; (AAm)(BIS) (copolymer), 25034-58-6; NaCl, 7647-14-5.

Density and Concentration Fluctuations in Plasticized Poly(cyclohexyl methacrylate)

G. Fytas* and G. Floudas

Research Center of Crete, P.O. Box 1527, 711 10 Iraklion, Crete, Greece

K. L. Ngai

Naval Research Laboratory, Washington D.C., 20375-5000. *Received May 22, 1989; Revised Manuscript Received August 7, 1989*

ABSTRACT: Polarized photon-correlation functions of high molecular weight plasticized PCHMA samples have been studied in the temperature range from near T_g to T_g + 150 K. The time-correlation function can measure both the density fluctuations caused by primary segmental relaxation and concentration fluctuations due to cooperative diffusion. It is the first time in a dynamic light-scattering experiment that both concentration and density correlation functions have been observed within the time window of the technique at the same temperature for a range of temperatures. The average primary relaxation times exhibit a strong temperature dependence with activation parameters experimentally the same for all plasticizer (DOP) concentrations. On the contrary, the activation parameters for the slow relaxation process were found to decrease with increasing DOP concentration. The coupling model, which is applicable to both segmental relaxation and cooperative diffusion, can explain this difference together with all accessorial features of the present experimental data.

Introduction

Photon-correlation spectroscopy (PCS) has been extensively utilized to study diffusion constants in polymer solutions and local relaxation processes in bulk amorphous polymers near and above T_g and only recently in the glassy state.[1] The dynamics of density and concentration fluctuations were studied by PCS for the first time in polydisperse poly(phenylmethylsiloxane) (PPMS).[2] The fast primary relaxation associated with the density fluctuations and the much slower q^2-dependent (with q^{-1} being the probing wavelength) diffusional mode were found to display vastly different temperature and pressure dependence.[3] This difference could be accounted for by the coupling model of relaxation.[4] However, the time-correlation functions for the fast density and slow concentration fluctuations in that system were recorded at different not overlapping temperature and pressure ranges, as their separation exceeds the time range accessible in present day digital correlators.

In this paper, we report PCS measurements of the density and concentration time-correlation functions for three plasticized PCHMA samples in the temperature range from near T_g to T_g + 150 K. The additive used was dioctyl phthalate (DOP) (actually bis(2-ethylhexyl) phthalate) with concentrations 5, 10, and 15 wt %. For the present system both relaxation processes fall within the correlator time regime (10–10^{-6} s) for temperatures between 90 and 125 °C. It is the first time in a dynamic light-scattering experiment that both concentration and density correlation functions have been observed within the time window of the technique at the same temperature for a range of temperatures.[25] This observation is not easily accomplished because of difficulties in the choice of systems that have significant contributions to light scattering from concentration fluctuations and also not too large a separation in the time scales of the relaxation times so that concentration and density fluctuations can be fitted into the experimentally accessible time window.

On the theoretical side, the coupling model, which is valid for considerations of both the density fluctuations caused by primary segmental relaxation and concentration fluctuations due to cooperative diffusion (also the terminal region for shear viscoelasticity),[5] has already been applied to explain the occurrence of two different temperature dependences of the corresponding relaxation times.[4] Although one may rationalize this difference by other means, it will be shown that the coupling model can explain this difference together with all accessorial features of the present experimental data.

Experimental Section

The time-correlation functions $G(q,t)$ of the polarized light scattered intensity at different temperatures (338–483 K) were measured at scattering angles of θ = 45, 90, and 150°. The light source was an argon ion laser (Spectra Physics 2020) operating

0024-9297/90/2223-1104$02.50/0

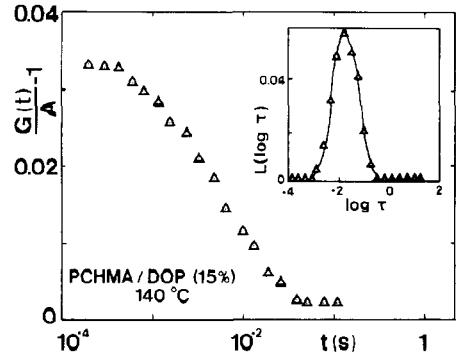

Figure 1. Measured net correlation function for the concentration fluctuations in PCHMA/DOP (15%) mixture at 140 °C and $\theta = 90°$. The corresponding retardation time spectrum, $L(\log \tau)$, plotted versus $\log \tau$, obtained from the inverse Laplace transform (ILT) analysis of the experimental correlation function is also shown.

at single mode at 488 nm with a stabilized power of 200 mW. The correlation functions $G(t)$ over 4.3 decades in time were measured with a 28-channel log-lin (Malvern K 7027) single-clipped correlator in one run. The PCHMA/DOP samples used in this study seem to display homodyne scattering as indicated from the low value (5.2 at 40 °C) of the Landau–Placzek Rayleigh–Brillouin intensity ratio. Hence, the desired normalized time-correlation function $g(q,t)$ is related to the measured $G(q,t)$ by

$$G(q,t) = A(1 + f|\alpha g(q,t)|^2) \quad (1)$$

where A is the base line measured at long delay times t, f the instrumental factor, and α is the fraction of the total scattered intensity associated with the slow density or concentration fluctuations.[6] Below 125 °C a time range larger than 4.3 decades is required to obtain $G(t)$. To encompass a larger dynamic range, two partially overlapping correlation functions measured in separate runs with different sample times were spliced together.[6] The amorphous PCHMA/DOP samples with 5%, 10%, and 15% DOP were carefully prepared by thermal polymerization and kindly provided by Dr. M. Stickler (Rohm, Darmstadt, FRG).

Data Analysis

We performed two types of analysis of the measured correlation functions. At high temperatures beyond 400 K the primary relaxation time becomes too fast to be measured by the correlator, which can monitor only the slow diffusional mode. In this case a single KWW decay function

$$g(q,t) = \exp[-(t/\tau^*(q))^{\beta_s}] \quad (2)$$

fits the experimental $(G(q,t)/A - 1)^{1/2}$, treating α, $\tau^*(q)$, and β_s as adjustable parameters. Figure 1 shows the net correlation function $(G(q,t)/A - 1)$ for the slow concentration fluctuations in PCHMA/DOP (15%) mixture at 140 °C. The corresponding retardation time spectrum,[7] $L(\log \tau)$, is also shown. The distribution parameter β_s is equal to 0.6 ± 0.07, 0.63 ± 0.1, and 0.68 ± 0.1, respectively, for the 5%, 10%, and 15% mixtures and is virtually independent of temperature. The average time $\tau_s = (\tau^*/\beta_s)\Gamma(1/\beta_s)$, with Γ being the gamma function, is q^2-dependent (Figure 2); $q = (4\pi/\lambda_0)n \sin(\theta/2)$, with λ_0 being the wavelength of laser light in vacuo and n the refractive index of the medium.

At the other extreme of low temperatures (<360 K) the slow diffusion process becomes very slow and cannot be detected within the long time limit of the correlator. Furthermore, since the intensity associated with this mode is relatively low, we treated the experimental $G(q,t)$ in the homodyne limit. Thus eq 1 along with eq 2 was used to represent the experimental correlation functions at low

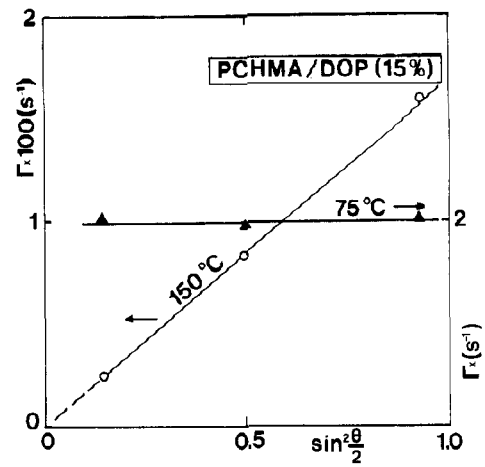

Figure 2. q^2-dependence of the relaxation time for the slow concentration fluctuations in PCHMA/DOP (15%) at 150 °C (○) and q-independence for the fast density fluctuations at 75 °C (▲).

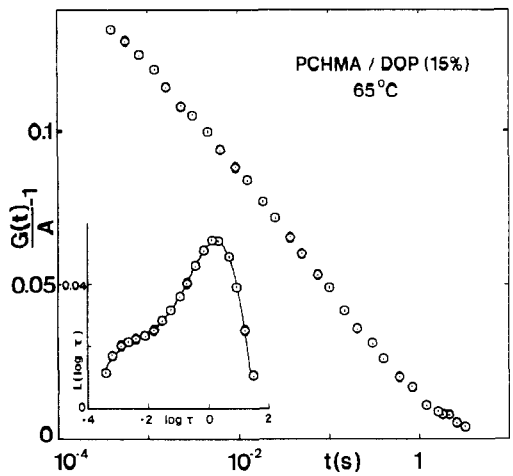

Figure 3. Measured net correlation function for the density fluctuations in PCHMA/DOP (15%) mixture at 65 °C. The corresponding retardation time spectrum, $L(\log \tau)$, is also given.

temperatures near T_g. Figure 3 shows a net correlation function of PCHMA/DOP (15%) mixture at 65 °C. The $L(\log \tau)$ is also shown. The distribution parameter β_f amounts to 0.4 ± 0.02, 0.38 ± 0.02, and 0.36 ± 0.02, respectively, for the 5%, 10%, and 15% DOP/PCHMA mixtures and is again insensitive to temperature variations. The average time τ_f for the fast local density fluctuations is q-independent (Figure 2) as expected for light scattering q's.

In the intermediate temperature range both processes can be detected within the time range of the correlator by using composite correlation functions. Such experimental correlation functions for the 15% samples at two temperatures and $\theta = 90°$ are shown in Figure 4. In this case of two simultaneous relaxation processes with distribution of decay rates, the $G(q,t)$ could be represented by a double KWW equation with six adjustable parameters. Instead of the use of a double KWW fit, we have chosen to analyze the $G(q,t)$ at all temperatures formally in terms of a continuous spectrum $L(\log \tau)$ of retardation times[7]

$$g(q,t) = \int_{-\infty}^{+\infty} d \ln \tau \, L(\ln \tau) \exp(-t/\tau(q)) \quad (3)$$

Figure 5 shows the results of the inverse Laplace transform (ILT) of the $(G(q,t)/A - 1)^{1/2}$ of Figure 4. The weak short time shoulder present also in bulk PCHMA[1] is probably related to the suppressed β-relaxation reported for

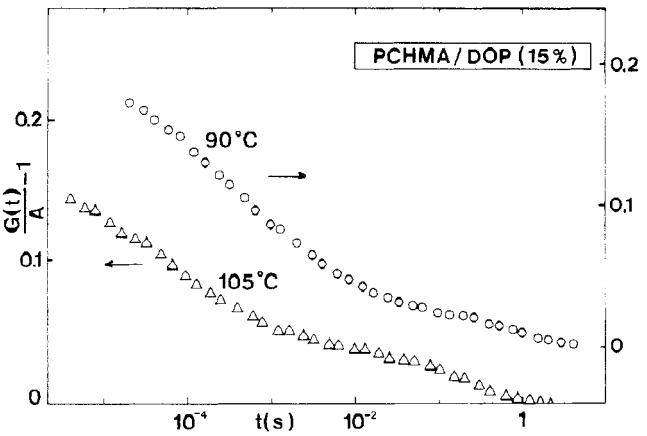

Figure 4. Measured composite net correlation functions at two temperatures for PCHMA/DOP (15%) mixture at $\theta = 90°$ (○, 90 °C; △, 105 °C).

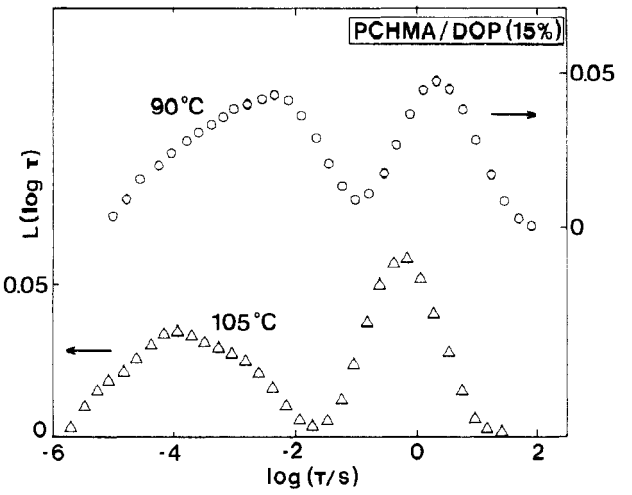

Figure 5. Comparison of the retardation time spectra, $L(\log \tau)$, of PCHMA/DOP (15%) mixture, at two temperatures, obtained from the inversion of the time correlation functions by using the ILT technique.

poly(alkyl methacrylates).[7] The pronounced β-peak in poly(methyl methacrylate)[8,9] is strongly depressed in PCHMA[1] due to the bulkier cyclohexyl group.[8]

Results

Using $L(\log \tau)$ to describe the distribution of retardation times, we write the average $\langle \log \tau \rangle$ (which is different from $\log \langle \tau \rangle$) as the first moment of the $L(\log \tau)$:

$$\langle \log \tau \rangle = \int_{-\infty}^{+\infty} \log \tau \, L(\log \tau) \, d \log \tau / \int_{-\infty}^{+\infty} L(\log \tau) \, d \log \tau \quad (4)$$

Figure 6 shows the variation of $\langle \log \tau \rangle$ of the different samples with temperatures equidistant from their T_g's for the fast primary relaxation and slow diffusion process. It is known that the VFTH equation

$$\langle \log \tau \rangle = \langle \log \tau \rangle_0 + B/(T - T_0) \quad (5)$$

represents well the temperature dependence of the primary relaxation times near T_g. In the VFTH equation $\langle \log \tau \rangle_0$, B, and T_0 are characteristic parameters. To determine unambiguously the values of these parameters from PCS data over a fairly narrow temperature range, we need to know T_0. In this context mechanical measurements over a broad temperature range will be very useful. Nevertheless, to examine the variation of B with DOP composition, we have used in the fit of eq 5 to the experimental times a fixed $T_0 = T_g - c_2$ as determined by computing T_g[10] (T_g = 359, 345, and 332 K for the 5%, 10%, and 15% DOP/PCHMA mixtures, respectively) and using $c_2 = 90$ K.[1] As is evident from Figure 6, the temperature dependences of the primary relaxation process for the bulk and plasticized PCHMA are almost undistinguishable when compared at temperatures equidistant from their T_g's. Consequently, the fit of eq 5 yields B = 1360 ± 120 K and $\langle \log \tau \rangle_0 = -13.5 \pm 1$ (in s) independent of the DOP composition. In contrary, from the fit of eq 5 to the slow diffusional relaxation process we obtain B and high-temperature intercepts $\langle \log \tau \rangle_0$, which show systematic variation with change in the concentration of the plasticizer. The values of B are 1260, 1080, and 940 K, respectively, for the mixtures with 5%, 10%, and 15% DOP whereas the corresponding $\langle \log \tau_s \rangle_0$ (in s) amounts to −9.1, −8.0, and −7.3.

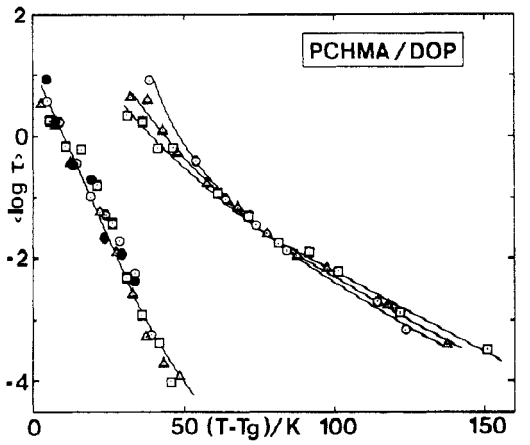

Figure 6. Plot of $\langle \log \tau \rangle$ for the fast and slow relaxation process in bulk (●) and plasticized PCHMA with DOP composition 5% (○), 10% (△), and 15% (□) versus $T - T_g(\varphi)$, where $T_g(\varphi)$ is the glass transition temperature of the plasticized polymer.[8]

Since we are primarily interested in the difference between the temperature dependences of the two processes, we follow a different approach. We have chosen the apparent activation energy

$$E = B\left(\frac{T}{T - T_0}\right)^2 2.303R \quad (6)$$

obtained from the Arrhenius fit of the experimental times in the same temperature range for both processes. In the temperature range 378–393 K the Arrhenius fit yields the apparent activation energies E_f = 61 ± 8 kcal/mol and E_s = 43 ± 4 kcal/mol for the fast and slow relaxation process, respectively, in the 10% DOP/PCHMA mixture. On the other hand, for the 15% mixture in the temperature range 363–378 K we obtain E_f = 69 ± 4 kcal/mol and E_s = 27 ± 2 kcal/mol.

Discussion

1. Slow Relaxation Process (Cooperative Diffusion). In Θ systems, which are the polymer solutions at very high polymer concentration, PCS studies are very limited.[11] The concentration correlation function $a_o g(q,t)$ can be written as[12]

$$a_o g(q,t) \sim \varphi_p g_m \exp(-\Gamma(q)t) \quad (7)$$

where φ_p is the monomer volume fraction, g_m is the number of monomers in a blob, and the relaxation rate Γ defines the cooperative diffusion coefficient, $D_c = \Gamma/(1 - \varphi_p)q^2$.

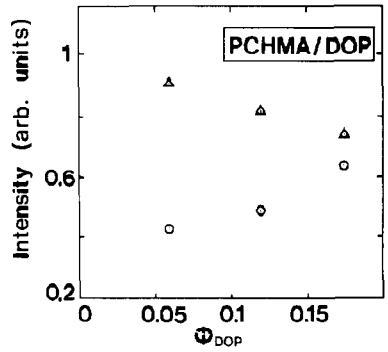

Figure 7. Scattering intensity from density (△) and concentration (○) fluctuations for the PCHMA/DOP mixtures obtained from the amplitude of the corresponding time correlation functions.

In Θ systems, $g_m \sim \varphi_p^{-2}$ and $D_c \sim \varphi_p$ as the restoring force for the concentration fluctuations is larger at higher polymer concentration. The scaling prediction (eq 7) for the fraction a_c of the total scattering intensity from concentration fluctuations is $a_c \sim \varphi_p^{-1}$. Figure 7 shows that $I_s = a_c I$ (with I being the total scattering intensity) is increasing with DOP concentration over the temperature range 130–210 °C in qualitative agreement with the theoretical prediction. On the other hand, the composition dependence of D_c is obscured by the strong composition dependent $T_g(\varphi)$. At temperatures far from T_g we indeed observed (Figure 6) systematically higher D_c values in the less plasticized samples.

The temperature dependence of D_c determined by that of the local friction coefficient $\zeta \sim \varphi_p^{-1}$ can probably be distorted by variation of the solvent quality with temperature. The solvent quality may affect the radius of a blob through excluded-volume interactions. However, the roughly temperature independent a_c as determined from the fit of eqs 1 and 2 to the experimental concentration correlation function suggests that D_c should exhibit a temperature dependence very close to that of ζ. The activation parameter, B, in eq 5 is therefore expected to be insensitive to variations of φ_p, which affects only the high-temperature intercept $\langle \log \tau \rangle_0$. In contrary, Figure 6 clearly shows that both B and $\langle \log \tau \rangle_0$ are increasing functions of φ_p. This behavior is to contrast with the temperature dependence of the fast relaxation process in the PCHMA/DOP system. An attempt to account for this difference will be discussed in the last section.

2. Fast Primary Relaxation (Local Density Fluctuations). Typical distribution $L(\log \tau)$ of retardation times for the density fluctuations are shown in Figures 3 and 5. The weak short time shoulder also reported for bulk PCHMA[11] is probably related to the depressed β-relaxation.[8] The average primary relaxation times listed in Table I exhibit strong temperature dependence described by eq 5 with activation parameters experimentally the same for all DOP concentrations. This situation is clearly shown in Figure 6 where all sets of the fast times $\langle \log \tau \rangle$ fall on a single curve.

The scattering intensity $I_f = \alpha_\rho I$, arising from density fluctuations shown in Figure 7, is found to decrease with DOP concentration over the temperature range 65–125 °C. The expected drop of I_f with decreasing polymer concentration is a composite decrease owing to the dilution effect and the change of the compressibility of the plasticized system. In this context hypersonic Brillouin data will be useful.

3. Slow and Fast Relaxation Modes. A. Principal Features of Experimental Data. Stated explicitly or implicitly throughout the text above are several outstanding but intriguing features of the experimental data on both the concentration fluctuation, due to cooperative diffusion, and the density fluctuation caused by the primary segmental relaxation. They are summarized and elaborated here as follows:

(a) The experimentally observed concentration correlation function $g_s(q,t)$ has the KWW form: $\exp[-(t/\tau_s^*(q))^{\beta_s}]$ and not the linear exponential form of eq 7. The exponent β_s appears to be increasing with DOP concentration; i.e., $\beta_s(\varphi_{DOP}) > \beta_s(\varphi'_{DOP})$ if $\varphi_{DOP} > \varphi'_{DOP}$. We have to remark, however, that the samples are polydisperse and polydispersity may account for at least part of the departure from linear exponential.

(b) The temperature dependence of the relaxation time, $\tau_s^*(q)$, as characterized by either B_s in eq 5 with $T_0 = T_g - c_2$ or the apparent activation energy, E_s, defined earlier, varies with DOP volume fraction, φ. Both B_s and E_s decrease with increasing φ; i.e., $B_s(\varphi) < B_s(\varphi')$ if $\varphi > \varphi'$. On the other hand, theoretical considerations based on blobs and scaling theory applied here predict no change of the temperature dependence of $\tau_s^*(q)$ with φ.

(c) The density fluctuation correlation function, $g_f(t)$, caused by segmental relaxations of the polymer chains has the KWW form $\exp[-(t/\tau_f^*)^{\beta_f}]$.

(d) It is the first time in a dynamic light-scattering experiment that both concentration and density correlation function have been observed within the time window of the technique at the same temperature for a range of temperatures. When the variations of τ_s^* and τ_f^* are compared with temperature within the common temperature range, it is clear that they have drastically different temperature dependences, with τ_f^* being the one having more strong variation with temperature. This is related to the difference in the temperature dependences of shift factors a_η and a_α for viscous deformation and glass-rubber (α–) relaxation, respectively, discovered first by D. J. Plazek[13–15] in his precise creep and creep recovery experiments and confirmed by others.[3,4,16–18] Our present photon-correlation spectroscopy data of PCHMA plasticized with 10% and 15% DOP provides unequivocal support to this. As mentioned earlier in the introduction, differences in both temperature and pressure depen-

Table I
Relaxation Times for Plasticized PCHMA[a]

	5% DOP		10% DOP		15% DOP	
T, °C	$\langle \log \tau_f \rangle$	$\langle \log \tau_s \rangle$	$\langle \log \tau_f \rangle$	$\langle \log \tau_s \rangle$	$\langle \log \tau_f \rangle$	$\langle \log \tau_s \rangle$
65					0.24	
70					−0.16	
75			0.56		−0.24	
80			0.17		−0.83	
85			−0.44		−1.44	
90	0.56				−2.33	0.35
95	0.26		−1.27		−2.93	0.24
100	−0.44		−1.92		−3.36	−0.22
105	−1.00		−2.58	0.63	−4.03	−0.22
110	−1.27		−3.25	0.60		
115	−1.71		−3.69	0.10		
120	−2.24		−3.92	−0.27		−0.92
125	−3.25	0.92				
130				−0.78		−1.33
140		−0.41		−1.16		−1.74
150		−1.04		−1.62		−1.91
160		−1.48		−1.97		−2.24
170		−1.88		−2.16		
180						−2.91
190				−2.76		
200		−2.72				
210		−3.17		−3.40		−3.51

[a] Mol wt of samples $\sim 1.0 \times 10^5$ g/mol; $M_w/M_n \approx 2$–3.

dences of τ_s^* and τ_f^* in PPMS have been deduced from extrapolations of data taken at nonoverlapping temperature and pressure range. Previous light-scattering work on amorphous polypropylene[18] has only detected density fluctuation, and we have to augment light-scattering data of segmental motion by the creep and creep recovery data in order to obtain a range of temperatures in which deformation and segmental relaxation have both been measured.

(e) The separation between the time scales τ_s^* and τ_f^* at temperature T is measured by the difference $\Delta\log\tau = \langle\log\tau_s^*(T)\rangle - \langle\log\tau_f^*(T)\rangle$. We shall compare the separations in PCHMA/DOP samples containing different amounts of DOP under the condition of constant $T - T_g$. The temperature T is chosen within the overlap of the temperature ranges of measurement of τ_s^* and τ_f^*. By inspection of Table I and Figure 6, it can be seen, starting from 15% DOP sample, that $\Delta\log\tau$ increases with decreasing DOP content. For example, at $T - T_g = 40$ K, which corresponds to 100 °C for 15%, 110 °C for 10%, and 125 °C for 5% DOP, $\Delta\log\tau$ equals 3.1 for 15%, 3.8 for 10%, and 4.2 for 5% DOP. The large increase of $\Delta\log\tau$ with decreasing DOP composition toward the total time window width of the correlator is one of the reasons that make observation of both concentration and density fluctuations at the same temperature increasingly more difficult. As we shall show, the coupling model, which can address both cooperative diffusion and segmental relaxation, is able to explain the decrease of $\Delta\log\tau$ with increasing DOP content as well as features a–d of the experimental data listed in this section.

It turns out that, in the framework of the coupling model, all the features are related in interesting ways to each other. For example, as to be discussed, we do expect β_s to increase with increase of DOP content (i.e., feature a). From this fact alone, we actually predict that B_s or E_s must decrease with increasing φ_{DOP} (i.e., feature b) and vice versa. Feature a together with feature c and the fact that $\beta_f(\varphi) < \beta_s(\varphi)$ are sufficient to predict feature d in a quantitative manner by the second relation of the coupling model, and remarkably also feature e.

B. Theoretical Explanation of the Experimental Features. In several previous investigations of similar nature, the coupling model[19,20] has been proven to be successful in providing a theoretical framework for understanding some of the features. In view of its prior success, naturally we continue to employ the coupling model to explain all the features a–e at one time. The essence and the predictions of the coupling model have appeared in various places[4,5,18–20] in the published literature, and there is no need for a repeated presentation here.

The weight average molecular weight, M_w, of the PCHMA is about 1.0×10^5 g/mol and $M_w/M_n \approx 2.5$. The critical molecular weight for entanglement M_c for PCHMA is not known to us. If it is comparable with $M_c = 31\,500$ for atactic PMMA, then the unplasticized PCHMA sample is entangled but not highly entangled. Moreover, owing to large polydispersity, it is possible that some chains are barely entangled or not even entangled. This situation for entanglement for chains in PCHMA means that, upon dilution by DOP, some chains may not be entangled. Even chains that remained entangled upon dilution may have their entanglement coupling reduced, because the entanglement spacing, M_e, increases with addition of DOP.

In the dynamic constraints dynamics version[20] of the coupling model, these situations for entanglement of chains here can be described summarily as mitigation of dynamic constraints[21,22] as the plasticizer is added. As dynamic constraints of chain entanglements are mitigated, the decelaration of molecular motion[18–20] is diminished, and the coupling parameter, n_s, decreases with DOP concentration. This is an expectation from the coupling model, which, as we shall see, is consistent with data. For later reference, we write this prediction out explicitly as

$$n_s(\varphi) < n_s(\varphi') \quad \text{if } \varphi > \varphi' \tag{8}$$

The polydispersity of the PCHMA/DOP systems introduces a distribution into the coupling parameter, n_s, and the relaxation time, τ_s^*, in the KWW correlation function

$$g_s(t) = \exp[-(t/\tau_s^*(\varphi))^{1-n_s(\varphi)}] \tag{9}$$

for chain relaxation after coupling by entanglements with other chains are considered. The relaxation time $\tau_s^*(\varphi)$ is obtained from the Rouse relaxation time, $\tau_{0s}(\varphi)$, by the "second" relation:

$$\tau_s^*(\varphi) = \{(1 - n_s(\varphi))\omega_c^{n_s(\varphi)}\tau_{0s}(\varphi)\}^{1/(1-n_s(\varphi))} \tag{10}$$

Thus, although the measured correlation function of concentration fluctuation, $g_s(t)$, is indeed of a KWW form (eq 2), the exponent β_s may not exactly reflect the distributed coupling parameter, n_s, through the relation $\beta_s = 1 - n_s$ because of the polydispersity. Any hope of a straightforward determination of the distribution of n_s through β_s of eq 2 is dashed by large polydispersity. This is not the case for n_f, which can be taken directly from $1 - \beta_f$ because the shape of the local density correlation function, $g_f(t)$, is independent of polydispersity. However, we can regard the coupling parameters, $n_s(\varphi)$, obtained from the experimental values

$$n_s(5\%) \approx 1 - \beta_s(5\%) = 0.40 \tag{11}$$

$$n_s(10\%) \approx 1 - \beta_s(10\%) = 0.37 \tag{12}$$

$$n_s(15\%) \approx 1 - \beta_s(15\%) = 0.32 \tag{13}$$

of the exponents only as an estimate of some average over the distribution. A similar remark applies also to the observed values $\tau_s^*(\varphi)$. Notwithstanding the fact that eqs 11–13 give only estimates of n_s, they satisfy the predicted inequality (eq 8). This semiquantitative comparison can be viewed as an explanation of feature a.

Feature b will be shown to follow as a consequence of the "second" relation of eq 10, where the temperature dependence of the primitive time τ_{0s} is given by a VFTH form (eq 5) with a φ-independent activation parameter, B_0. Then the temperature dependence of τ_s^* has another VFTH form characterized by the parameter $B_s^*(\varphi)$ given by

$$B_s^*(\varphi) = B_0/(1 - n_s(\varphi)) \tag{14}$$

Thus, from this expression for $B_s^*(\varphi)$ and the inequality (eq 8) between the $n_s(\varphi)$'s we predict

$$B_s^*(\varphi) < B_s^*(\varphi') \quad \text{if } \varphi > \varphi' \tag{15}$$

We see that this prediction is in accord with the decrease of the experimental values B_s (to be identified with B_s^* of eq 14) with φ, i.e., 1260, 1080, and 940 K, respectively, for 5%, 10%, and 15% DOP. Polydispersity renders the determination of $n_s(\varphi)$ from β_s uncertain, otherwise B_0 can be deduced from eq 14 unambiguously. If the temperature dependence of τ_{0s} is represented instead by an Arrhenius form with activation energy E_0 for a limited temperature region such as the overlap of measurement temperatures of concentration and density fluctuations,

then in analogy to eq 14

$$E_s^* = E_0/(1 - n_s(\varphi)) \quad (16)$$

When combined with inequality (eq 8) the last equation predicts

$$E_s^*(\varphi) < E_s^*(\varphi') \quad \text{if } \varphi > \varphi' \quad (17)$$

which is in agreement with the larger experimental apparent activation energy E_s of about 40 kcal/mol for the 10% DOP sample and about 30 kcal/mol for the 15% DOP sample.

Feature d has been explained[4,5,18,23] in various contexts, including shear viscoelasticity,[5,13-16] dielectric relaxation,[24] and photon-correlation spectroscopy,[3,18] by the difference in the coupling parameters n_s and n_f for the two processes. There is a corresponding "second" relation (eq 10) for the relaxation time, τ_f^*, relating it to the primitive relaxation time, τ_{0f}, of conformational transition in a chain. The same friction factor, ζ_0, determines the temperature dependence of both τ_{0s} and τ_{0f}. However, raising this same temperature dependence to the different powers $1/(1 - n_s)$ and $1/(1 - n_f)$ (eq 10) will generate two different temperature dependences for τ_s^* (eq 14) and τ_f^*, respectively. When eq 16 is applied for the slow and fast relaxation process, a relation between E_s^* and E_f^* easily follows:

$$(1 - n_f)E_f^* = (1 - n_s)E_s^* \quad (18)$$

To test the latter relation against data, we take $E_f^* = 65$ kcal/mol, the average over the apparent activation energies of 10% and 15% DOP/PCHMA. Then, for 10% DOP with $\beta_f = 0.38$ and $\beta_s = 0.63$, we deduce from eq 18 the value of 39.2 kcal/mol for E_s^*, which is comparable to the experimental value of 43 ± 4 kcal/mol. Similarily, for 15% DOP, with $\beta_f = 0.36$ and $\beta_s = 0.68$ we deduce $E_s^* = 34.4$ kcal/mol as compared with 27 ± 2 kcal/mol. There is semiquantitative agreement between prediction of eq 18 and experimental data in each case.

Finally, we address feature e. As demonstrated in Figure 6, after adjusting $T_0(\varphi)$ to $T_g(\varphi)$ the data points for the segmental times $\tau_f^*(\varphi)$ for different φ fall nicely on a master curve when plotted against $T - T_0(\varphi)$ or equivalently against $T - T_g(\varphi)$. In the context of the coupling model, via eq 10 (for the fast mode), this is achieved because both $n_f(\varphi)$ and τ_{0f} are independent of φ. This is true for τ_{0f} because an isofriction condition is satisfied at constant $T - T_g(\varphi)$, and isofriction condition means ζ_0 and hence τ_{0f} as well as τ_{0s} are independent of φ. The expression in eq 10 can be rewritten:

$$\tau_s^*(\varphi) = \{\omega_c \tau_{0s}\}^{n_s(\varphi)/(1-n_s(\varphi))}[1 - n_s(\varphi)]^{1/(1-n_s(\varphi))} \quad (10')$$

The dominant factor in curly brackets raised to the power $n_s(\varphi)/(1 - n_s(\varphi))$ increases with increasing $n_s(\varphi)$ because $\omega_c \tau_{0s} \gg 1$ and the exponent $n_s(\varphi)/(1 - n_s(\varphi))$ is an increasing function of $n_s(\varphi)$. If we recall from experimental data that $n_s(\varphi)$ decreases with increasing φ, then the results here show that, at constant $T - T_g(\varphi)$, $\tau_s^*(\varphi)$ decreases with increasing φ. Since $\tau_f^*(\varphi)$ is independent of φ under the same condition of constant $T - T_g(\varphi)$, it follows that $\Delta \log \tau = \langle \log \tau_s^* \rangle - \langle \log \tau_f^* \rangle$ decreases with increasing φ, i.e., feature e.

Conclusions

In this work we examine the dynamics of the fast primary relaxation due to local density fluctuations and slow relaxation process due to cooperative diffusion in a plasticized PCHMA system above T_g. Both density and concentration correlation functions have been observed within the time window of the technique at the same temperature for a range of temperatures, making possible comparison between τ_s^* and τ_f^* under the same conditions. τ_s^* and τ_f^* have drastically different temperature dependences, with τ_f^* having more strong variation with temperature. All three plasticized PCHMA samples show the same temperature dependence of τ_f^* with that of the bulk polymer at temperatures equidistant from their T_g's. The temperature dependence of the relaxation time, τ_s^*, as characterized by the activation energy, B_s, or the apparent activation energy, E_s, decreases with increasing DOP concentration. These outstanding features of the experimental data present challenges to any model of segmental mode relaxation and cooperative chain diffusion for explanations. In this paper we examine only the coupling model which is applicable to both segmental relaxation and chain diffusion. We found that this model can explain all the features identified.

Acknowledgment. The financial support of the RCC and NRL is gratefully acknowledged. We thank also Dr. M. Stickler of Rohm, Darmstadt, FRG, for providing us with the plasticized PCHMA samples.

References and Notes

(1) Fytas, G. *Macromolecules* **1989**, *22*, 211.
(2) Fytas, G.; Dorfmuller, T.; Lin, Y. H.; Chu, B. *Macromolecules* **1981**, *14*, 1088.
(3) Fytas, G.; Dorfmuller, T.; Chu, B. *J. Polym. Sci., Polym. Phys. Ed.* **1984**, *22*, 1471.
(4) Ngai, K. L.; Fytas, G. *J. Polym. Sci., Polym. Phys. Ed.* **1986**, *24*, 1683.
(5) Ngai, K. L.; Plazek, D. J. *J. Polym. Sci., Polym. Phys. Ed.* **1986**, *24*, 619.
(6) Wang, C. H.; Fytas, G.; Lilge, D.; Dorfmuller, T. *Macromolecules* **1981**, *14*, 1363.
(7) Hagenah, J. U.; Meier, G.; Fytas, G.; Fischer, E. W. *Polym. J.* **1987**, *19*, 441.
(8) Heijboer, J. *Int. J. Polym. Mater.* **1977**, *6*, 11.
(9) Fytas, G.; Wang, C. H.; Fischer, E. W. *Macromolecules* **1988**, *21*, 2953.
(10) Kalachandra, S.; Turner, D. T. *J. Polym. Sci., Polym. Phys.* **1987**, *25*, 1971.
(11) Hwang, D.; Cohen, C. *Macromolecules* **1984**, *17*, 2890.
(12) See, for example: de Gennes, P.-G. *Scaling Concepts in Polymer Physics*; Cornell University: Ithaca, NY, 1979; Chapter VII. Schaefer, D. W.; Han, C. C. In *Dynamic Light Scattering*; Pecora, R., Ed.; Plenum Press: New York, 1985; p 181.
(13) Plazek, D. J. *J. Phys. Chem.* **1965**, *69*, 3480; *Polym. J.* **1980**, *12*, 43.
(14) Plazek, D. J. *J. Polym. Sci., Polym. Phys. Ed.* **1982**, *20*, 729.
(15) Plazek, D. L.; Plazek, D. J. Macromolecules **1983**, *16*, 1469.
(16) Cavaile, J. Y.; Perez, J.; Jourdan, C.; Johari, G. P. *J. Polym. Sci., Polym. Phys. Ed.* **1987**, *25*, 1847.
(17) Alberdi, J. M.; Alegria, A.; Macho, E.; Colmenero, J. *Polym. Bull. (Berlin)* **1987**, *18*, 39.
(18) Fytas, G.; Ngai, K. L. *Macromolecules* **1988**, *21*, 804.
(19) For a review, see: Ngai, K. L.; Rendell, R. W.; Rajagopal, A. K.; Teitler, S. *Ann. N.Y. Acad. Sci.* **1986**, *484*, 150 and references therein.
(20) Ngai, K. L.; Rajagopal, A. K.; Teitler, S. *J. Chem. Phys.* **1988**, *88*, 5086.
(21) Ngai, K. L.; Lodge, T. P. *ACS Polym. Prepr.*, in press.
(22) Ngai, K. L.; Lodge, T. P., submitted for publication in *J. Chem. Phys.*
(23) Ngai, K. L.; Rendell, R. W. *ACS Polym. Prepr.*, in press.
(24) Boese, D.; Kremer, F. *Makromol. Chem., Rapid Commun.* **1988**, *9*, 367.
(25) In a mixture of glass-forming liquids of small molecules B. Gerharz, G. Meier, and E. W. Fischer of MPI at Mainz, FRG, have also observed density and concentration fluctuations at few temperatures.

Registry No. PCHMA, 25768-50-7; DOP, 117-81-7.